

Physicochemical changes in phosphorylase kinase induced by its cationic activator Mg^{2+}

Weiya Liu, Owen W. Nadeau, Jessica Sage, and Gerald M. Carlson*

Department of Biochemistry and Molecular Biology, University of Kansas Medical Center, Kansas City, Kansas 66160

Received 2 November 2012; Revised 15 January 2013; Accepted 17 January 2013

DOI: 10.1002/pro.2226

Published online 29 January 2013 proteinscience.org

Abstract: For over four decades free Mg^{2+} ions, that is, those in excess of MgATP, have been reported to affect a wide variety of properties of phosphorylase kinase (PhK), including its affinity for other molecules, proteolysis, chemical crosslinking, phosphorylation, binding to certain monoclonal antibodies, and activity, which is stimulated. Additionally, for over three decades Mg^{2+} has been known to act synergistically with Ca^{2+} , another divalent activator of PhK, to affect even more properties of the enzyme. During all of this time, however, no study has been performed to determine the overall effects of free Mg^{2+} ions on the physical properties of PhK, even though the effects of Ca^{2+} ions on PhK's properties are well documented. In this study, changes in the physicochemical properties of PhK induced by Mg^{2+} under nonactivating (pH 6.8) and activating (pH 8.2) conditions were investigated by circular dichroism spectroscopy, zeta potential analyses, dynamic light scattering, second derivative UV absorption, negative stain electron microscopy, and differential chemical crosslinking. The effects of the activator Mg^{2+} on some of the properties of PhK measured by these techniques were found to be quite different at the two pH values, and displayed both differences and similarities with the effects previously reported to be induced by the activator Ca^{2+} (Liu *et al.*, *Protein Sci* 2008;17:2111–2119). The similarities may reflect the fact that both cations are activators, and foremost among their similarities is the dramatically less negative zeta potential induced by their binding to PhK.

Keywords: phosphorylase kinase; activation; Mg^{2+} ; Ca^{2+} ; dimerization; zeta potential; dynamic light scattering; electron microscopy; differential crosslinking; dibromobimane

Introduction

Phosphorylase kinase (PhK) is the first protein kinase to be characterized,¹ and remains one of the largest and most complex members of that superfamily (review²). The enzyme from rabbit skeletal muscle,

the subject of this study and all of those listed in Table I,^{3–24} has a mass of 1.3 MDa and is composed of four copies each of four different subunits, $(\alpha\beta\gamma\delta)_4$. The γ subunit (44.7 kDa) is the catalytic kinase, whereas the α (138.4 kDa), β (125.2 kDa), and δ (16.7 kDa) subunits are regulatory. Ca^{2+} ions are obligatory activators of PhK and exert their effect through the δ subunit, which is tightly bound intrinsic calmodulin. The binding of Ca^{2+} to PhK induces a large number of physical changes in the complex that have been thoroughly characterized.^{25–27} A second divalent cation that has been known for more than forty years to affect PhK is free Mg^{2+} , distinct from MgATP. Although its effects are diverse and pronounced (Table I), virtually nothing is known regarding the physical changes the enzyme undergoes when Mg^{2+} is bound, which is the subject of this study.

Abbreviations: apo-PhK, PhK in 0.2 mM EGTA; DFDNB, 1,5-difluoro-2,4-dinitrobenzene; dibromobimane, (4,6-bis(bromoethyl)-3,7-dimethyl-1,5-diazabicyclo[3.3.0]octa-3,6-diene-2,8-dione); DLS, dynamic light scattering; Mg^{2+} -PhK, PhK in 4.2 mM $Mg(CH_3CO_2)_2$ + 0.2 mM EGTA; PhK, phosphorylase kinase.

Grant sponsor: N.I.H.; Grant number: DK32953.

*Correspondence to: Gerald M. Carlson, Department of Biochemistry and Molecular Biology, University of Kansas Medical Center, 1083 KLSIC, Mail Stop 3030, 3901 Rainbow Blvd., Kansas City, KS 66160. E-mail: gcarlson@kumc.edu

Table I. Effects of Free Mg^{2+} Ions on Nonactivated PhK

Phk	Effect	References
<i>Kinase Activity</i>		
6.8	Time-dependent activation prior to assay ^a	3
6.8	Time-dependent activation prior to assay when incubated with phosphorylase ^a	4
6.8	Stimulates when in excess over MgATP	5,6
8.2	Stimulates when in excess over MgATP	6,7
<i>Affinity for Interacting Molecules</i>		
6.8	Alters affinity for Ca^{2+} plus induces new Ca^{2+} binding sites	8
7.5	Increases affinity for glycogen phosphorylase	9
<i>Effects on Specific Subunits</i>		
8.2	Increased $\beta\beta 1$ and $\alpha\gamma$ conjugates and decreased $\beta\gamma\gamma$ in crosslinking by 4-phenyl-1,2,4-triazoline-3,5-dione	10
6.8	Protects β subunit from trypsinolysis	11
6.8	Increased binding of mAb $\gamma 79$ to free γ subunit and to PhK	12
6.8	Increased binding of mAb $\gamma 88$ and mAb γ to PhK	13
6.8	Increased phosphorylation of α subunit at high $[Mg^{2+}]$ by two distinct protein kinases	14,15
<i>Synergistic Effects in Concert with Ca^{2+} Ions</i>		
6.8	Promotes self-association of PhK	16–18
6.8	Incubation prior to assays activates kinase	19
6.8	Promotes formation of β - β dimers in crosslinking by 1,5-difluoro-2,4-dinitrobenzene (DFDNB)	20
6.8	Incubation prior to assays induces an EGTA-insensitive activity	21
6.8/7.0	Enhances binding to glycogen	22–24

^a Without divalent cation chelator.

Besides acting by itself, Mg^{2+} also acts synergistically with Ca^{2+} to induce a large number of changes in PhK (Table I), and these effects have been shown in nearly all cases to be time-dependent over the course of minutes. The other studies cited in Table I using Mg^{2+} alone, did not take possible time-dependence into account, with the exception of the first two in the table; however, neither of those utilized a divalent cation chelator, thus contaminating free Ca^{2+} ions may have been present in varying amounts in their experiments, possibly leading to a time-dependent Ca^{2+}/Mg^{2+} synergism. Consequently, the current study on the physical effects of Mg^{2+} on PhK also examined potential time-dependence.

Besides its activation through phosphorylation by other protein kinases or itself, PhK can be activated by a variety of other mechanisms and effectors. In all cases this leads to a large increase in its catalytic activity at pH 6.8, with only a slight increase at pH 8.2,^{2,28} thus the ratio of activity at these pH values has been traditionally used as an index of PhK's activation. In fact, simply increasing the pH over the same range in assays, itself activates the kinase. This pH effect is due to deprotonation of residues on PhK's large regulatory α or β subunits, as the catalytic activities of the isolated γ subunit and a $\gamma\delta$ dimer are the same at both pH values.^{29,30} It can be noted that nearly all the studies of Table I were performed at one or both of these pH values; likewise, the effects of Mg^{2+} ions on PhK were compared at these two pH values in this cur-

rent study. As will be shown, the effects of Mg^{2+} on the physical properties of PhK are different at the two pH values, as is the time-dependence of those Mg^{2+} -induced changes.

Results

For all of the experimental approaches used in this study, except microscopy and crosslinking, the concentration of PhK was kept constant at 0.10 mg/mL, allowing comparison of not only the Mg^{2+} -induced changes observed using the different techniques herein but also comparison with our previously observed Ca^{2+} -induced biophysical changes, which were also measured at this concentration of PhK.^{25,26}

Circular dichroism spectroscopy

Circular dichroism (CD) was used to investigate changes in the secondary structure of PhK induced by the binding of Mg^{2+} ions. At pH 6.8 the peak of Mg^{2+} -PhK located at ~ 208 nm was shifted to higher wavelengths with increased incubation time, concomitant with a decrease in the intensity of the CD signal, whereas the ellipticity at 222 nm showed only a small decrease without any change in the peak position [Fig. 1(A)]. The CD spectra showed little change in the first 2 min, the minimum time required for most of the biophysical measurements in this study: slightly less negative ellipticity at 208 nm and no change at 222 nm [Fig. 1(A, inset)]. The CD spectra of Mg^{2+} -PhK observed at pH 8.2 were very different from those at pH 6.8, as neither the

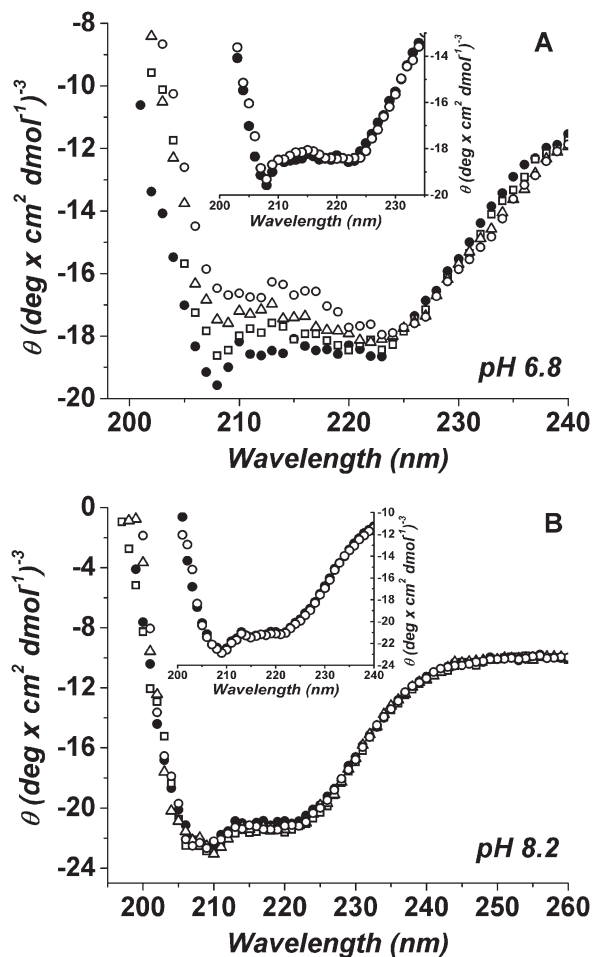


Figure 1. CD spectra of Mg^{2+} -PhK at different incubation times at pH 6.8 (A) or 8.2 (B). CD spectra were recorded from 190 to 260 nm and are presented as the average of three consecutive 30-s scans. The incubation times with Mg^{2+} displayed here are 10 min (□), 20 min (△) and 30 min (○), shown with the zero-time control without Mg^{2+} (●). Each inset shows the CD spectra of PhK after 2-min incubation with Mg^{2+} (○) or without (●).

peak position nor the peak intensity of PhK showed much change over time [Fig. 1(B)].

As previously discussed with respect to PhK,^{25,26} the ratio of negative ellipticity at 222 nm to 208 nm is an index of the extent of interaction between α -helices and β -sheets.^{31–35} Upon the addition of Mg^{2+} at pH 6.8, the $\theta_{222}/\theta_{208}$ ratio remained unchanged during the first 2 min, then linearly increased with time, exceeding unity at ~ 12 min [Fig. 2(A)]. In contrast, at pH 8.2 the $\theta_{222}/\theta_{208}$ ratio in the presence of Mg^{2+} showed little change during the experimental time period [Fig. 2(B)]. As controls, apo-PhK was examined at both pH values and showed no change in the $\theta_{222}/\theta_{208}$ ratio over time [Fig. 2(A,B)].

Electrostatic surface charge/zeta potential

Zeta potential measurements, obtained by analyzing the shear surface electric potential of colloidal particles in solution, provide estimates of effective sur-

face charge.^{36,37} In previous studies on PhK, an increase in the $\theta_{222}/\theta_{208}$ ratio and change in the surface charge to less negative were found to correlate with the activation state of the enzyme.²⁶ In this study, by using phase analysis light scattering, the zeta potentials of apo-PhK and Mg^{2+} -PhK were measured as a function of time at pH 6.8 and 8.2 (Fig. 3). At pH 6.8, the apo-PhK had the most negative zeta potential ($\sim -32 \pm 2$ mV), but upon addition of Mg^{2+} ions, it rapidly became less negative ($\sim -6 \pm 1$ mV) and stayed at that level throughout the experiment. Increasing the pH from 6.8 to 8.2 also caused the zeta potential of PhK to become less negative ($\sim -10 \pm 1$ mV); however, the addition of Mg^{2+} did not induce further change. None of these four PhK species showed any time-dependent changes in zeta potential following the first measurement at 2 min.

Optical density measurements

Besides the possibility of conformational changes altering contacts between α -helices and β -sheets, leading to peak position changes and a decrease in

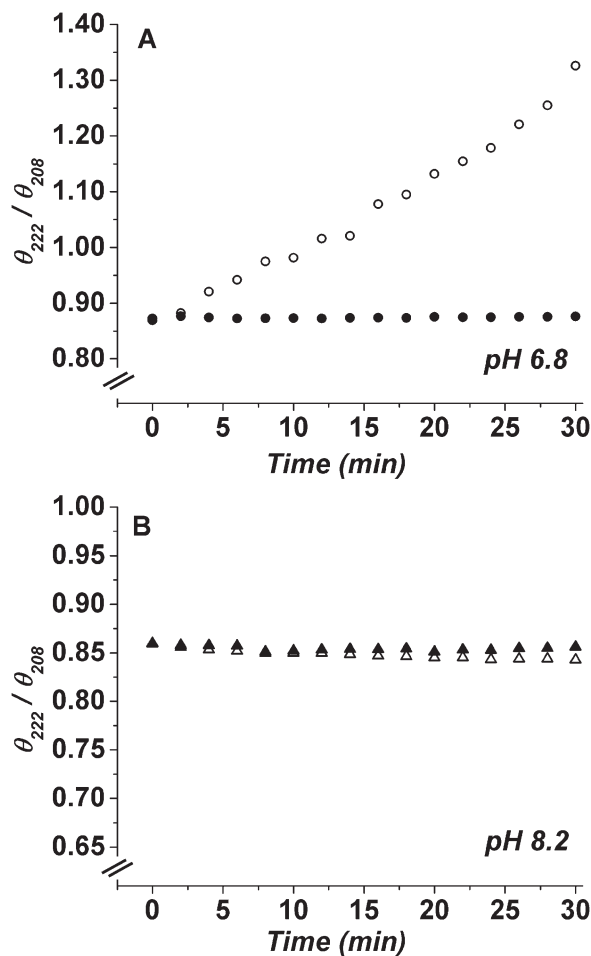


Figure 2. The $\theta_{222}/\theta_{208}$ (CD) ratios as a function of time for apo-PhK (●,▲) and Mg^{2+} -PhK (○,△) at pH 6.8 (A) or pH 8.2 (B).

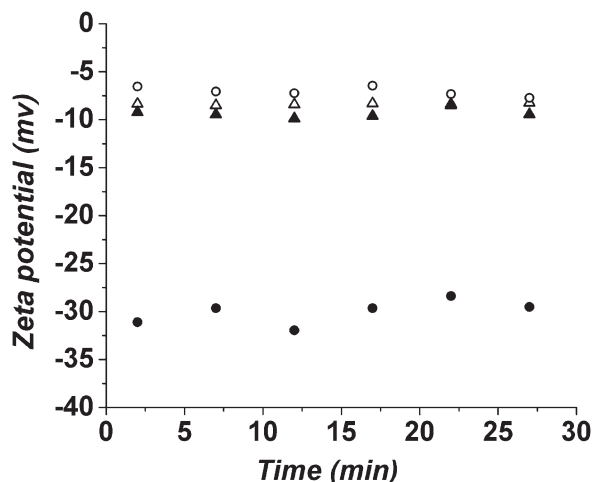


Figure 3. Zeta potential values as a function of time for apo-PhK (●) and Mg²⁺-PhK (○) at pH 6.8, and for apo-PhK (▲) and Mg²⁺-PhK (△) at pH 8.2.

peak intensity in the CD spectra, self-association of the protein could have similar effects.^{38–40} Thus, the time-dependent decrease in ellipticity of the 208 nm peak of Mg²⁺-PhK at pH 6.8, along with the time-dependent increase in its $\theta_{222}/\theta_{208}$ ratio [Figs. 1(A) and 2(A)], could be due in part to a time-dependent aggregation of PhK upon its binding of Mg²⁺. To assess PhK's potential aggregation, its optical density at 360 nm was monitored over time following the addition of Mg²⁺ ions.⁴¹ The OD values of Mg²⁺-PhK at pH 6.8 did not change much in the first 2 min, suggesting that extensive aggregation did not occur during this time period; but after that, a slow time-dependent aggregation began and did not reach a plateau during 2 hr (Fig. 4). In contrast to pH 6.8, there were no changes in the OD values of PhK upon the binding of Mg²⁺ at pH 8.2 (Fig. 4), which conforms with our CD results (Fig. 1).

Dynamic light scattering

The results shown in Figure 4 prompted us to use dynamic light scattering (DLS) to evaluate the potential self-association of PhK during 30-min incubations. At pH 6.8, apo-PhK showed only one population with a hydrodynamic diameter of ~32 nm [Fig. 5(A)]. This size is consistent with the dimensions of the PhK complex obtained through electron microscopy⁴² and small-angle X-ray scattering,⁴³ and it did not change over the course of the experiment. In contrast, after short incubations Mg²⁺-PhK displayed two populations, with hydrodynamic diameters of ~60 and ~250 nm, that reached a ratio of 60:40, respectively, after 30 min [Fig. 5(B)]. The size of the 60 nm particles is consistent with dimers of the PhK hexadecamer. At pH 8.2, apo-PhK had only one population, with an apparent hydrodynamic diameter of ~27 nm [Fig. 5(C)], or smaller than observed at pH 6.8. The binding of Mg²⁺ at pH 8.2

increased the apparent size of PhK from 27 to 32 nm [Fig. 5(D)], but without aggregation occurring. At pH 8.2, the apparent hydrodynamic diameters of both apo-PhK and Mg²⁺-PhK stayed constant during the 30-min incubation, conforming with the CD and OD studies.

Electron microscopy

DLS results suggested that when incubated with Mg²⁺ at pH 6.8, PhK began to form dimers of hexadecamers in a short time; so, electron microscopy of negatively stained particles was used to evaluate this possibility. Control micrographs of negatively stained apo-PhK showed images of the molecule in the typical orientations that have been previously characterized for hexadecameric single particles [Fig. 6(A)].⁴⁴ To visualize Mg²⁺-PhK, we limited PhK's incubation time with Mg²⁺ to 30 s, hoping to avoid aggregates being present on the grids. The images of Mg²⁺-PhK clearly showed an enrichment of PhK dimers, with two molecules of PhK arranged in several different orientations [Fig. 6(B)]. Over one thousand apo-PhK and Mg²⁺-PhK particles were analyzed from multiple grids by visual inspection of WEB displays,⁴⁵ with all monomer and dimer particles selected and counted; the percentage of dimers to monomers observed was 4.3% for apo-PhK and 25.1% for Mg²⁺-PhK.

Second derivative UV absorption spectroscopy

Because DLS suggested that Mg²⁺ induces some structural changes in PhK at pH 8.2 (Fig. 5), without causing aggregation, second derivative UV absorption spectroscopy was used to monitor any changes in structure induced by Mg²⁺ at that pH value. PhK possesses a large number of aromatic residues (428 Phe, 460 Tyr, and 124 Trp), and changes in the microenvironment of these residues induce changes in their spectral characteristics, thus

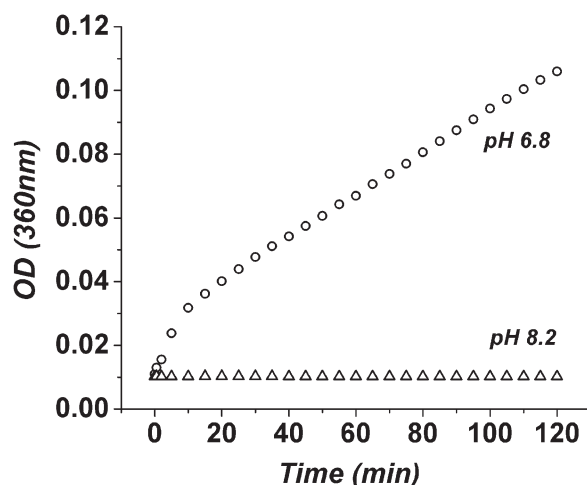


Figure 4. The optical density at 360 nm as a function of time for Mg²⁺-PhK at pH 6.8 (○) and 8.2 (△).

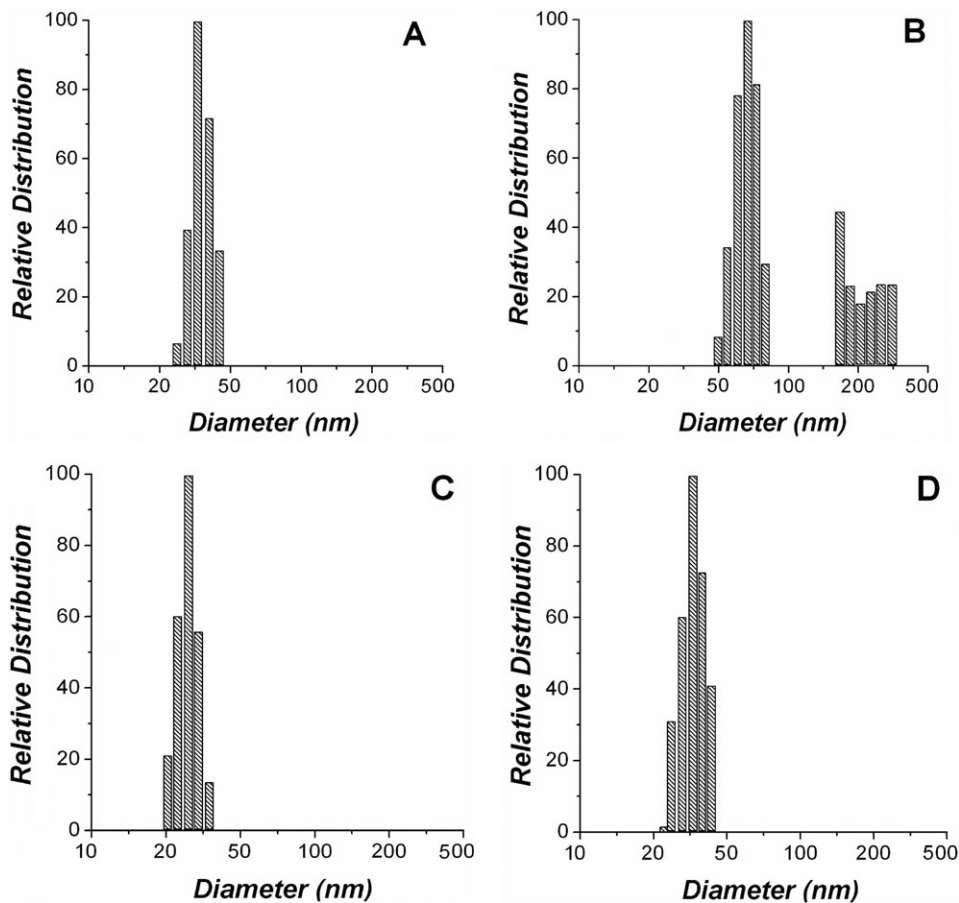


Figure 5. Distribution of PhK's particles size after 30-min incubation with Mg^{2+} ions. (A) apo-PhK at pH 6.8, (B) Mg^{2+} -PhK at pH 6.8, (C) apo-PhK at pH 8.2, and (D) Mg^{2+} -PhK at pH 8.2.

providing a means to monitor changes in structure.⁴⁶ The second derivative spectra of apo-PhK showed six peaks with the following assignments: Phe (~253 and 259 nm), Tyr (~269 and ~277 nm),

an overlapping Tyr/Trp signal (285 nm), and Trp (292 nm) (Fig. 7). Upon Mg^{2+} binding, peak shifts occurred only for those peaks assigned to Tyr residues, with the Tyr peaks at 269 and 277 nm being

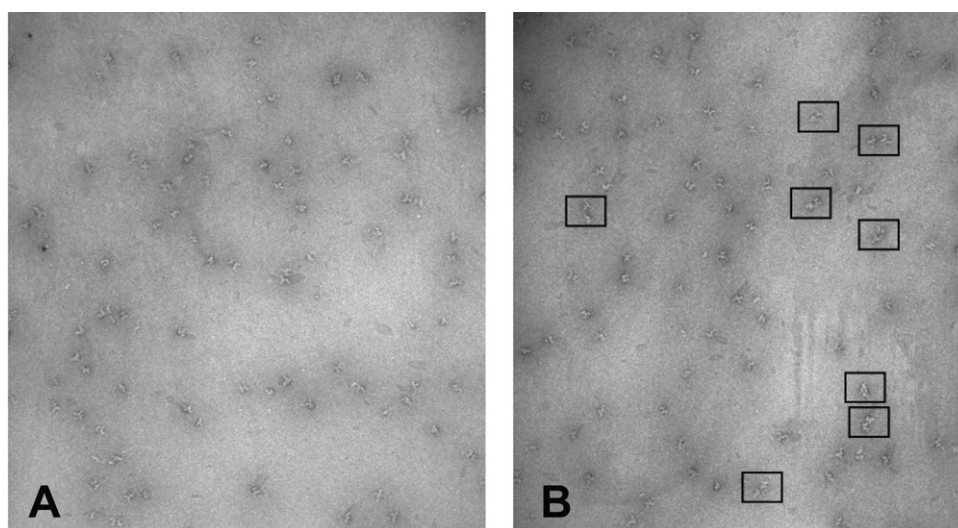


Figure 6. Negatively stained fields of PhK containing a mixture of orientations of the complex. (A) apo-PhK at pH 6.8, (B) Mg^{2+} -PhK at pH 6.8 after 30-s incubation with Mg^{2+} . The boxes around particles in the field designate typical examples of PhK dimers.

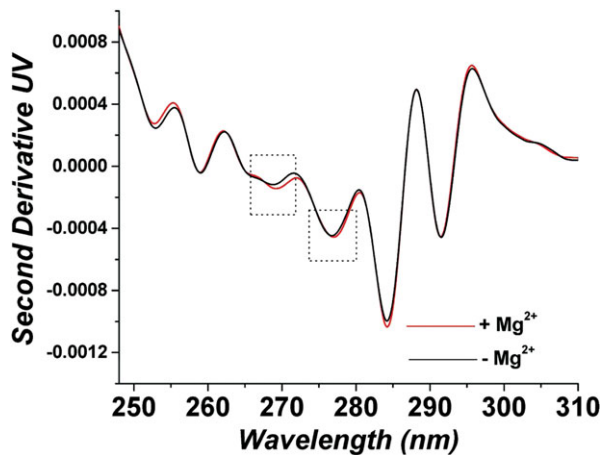


Figure 7. High-resolution second derivative UV spectroscopy of PhK after 30-min incubation \pm Mg^{2+} at pH 8.2.

shifted to longer wavelengths (Fig. 7), consistent with these residues being moved to a more apolar environment.⁴⁷ Presumably, the burial of tyrosyl residues is associated with the Mg^{2+} -induced structural changes at pH 8.2 that are detected by DLS.

Differential crosslinking of PhK

To further investigate potential conformational changes induced in PhK by Mg^{2+} at pH 6.8, a cross-linking screen was carried out to identify reagents capable of very rapidly crosslinking subunits within the complex at this pH value. To enhance sensitivity and determine subunit composition of crosslinked conjugates, while still retaining screening simplicity, products were initially analyzed by Western blotting against subunit-specific monoclonal antibodies after a fixed-time (2 min) of incubation \pm Mg^{2+} , followed by a fixed-time (1 min) of crosslinking. Dibromobimane (4,6-bis(bromoethyl)-3,7-dimethyl-1,5-diazabicyclo[3.3.0]octa-3,6-diene-2,8-dione), a thiol-selective crosslinker having a short span (4.9 Å), fulfilled these criteria by rapidly promoting intramolecular crosslinking that was different \pm Mg^{2+} [Fig 8(A)]. This reagent, which has not been previously used to crosslink PhK, targeted predominantly the β and γ subunits, with Mg^{2+} either stimulating or inducing formation of heteromeric conjugates of intermediate mass containing those subunits: $\beta\gamma\gamma$ (mass_{Exp} = 228 kDa, 6.5% error), $\beta\gamma\gamma_i$ (apparent intrasubunit cross-linked form of $\beta\gamma\gamma$; mass_{Exp} = 197 kDa, 8.0% error;

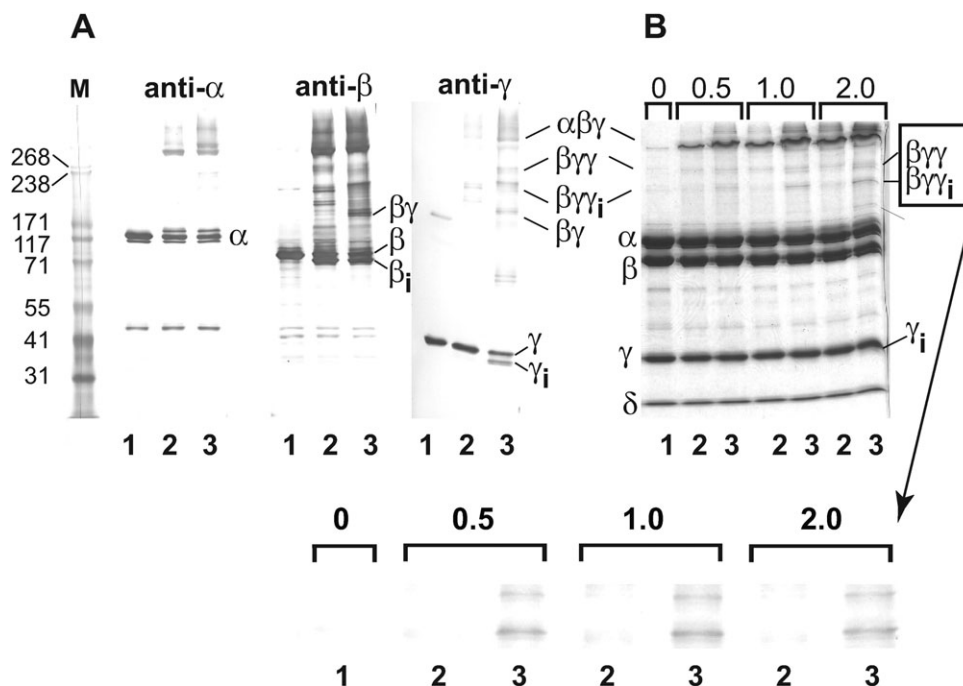


Figure 8. Mg^{2+} -dependent crosslinking of PhK with dibromobimane at pH 6.8. (A) Native PhK (Lane 1—control) was crosslinked with dibromobimane for 1.0 min following incubation for 2.0 min in the absence (Lane 2) and presence (Lane 3) of Mg^{2+} . The crosslinking was quenched by addition of SDS buffer. Following electrophoresis, all conjugates were identified by their apparent masses and cross reactivities against subunit-specific mAbs using previously described methods.⁵⁷ No conjugates containing the intrinsic calmodulin (δ) subunit were detected in Western blots with the anti-calmodulin mAb (data not shown). Subunits and all conjugates formed by crosslinking are indicated both to the left and right of the blots and gel, with intramolecular crosslinking of species indicated by subscript i. (B) Crosslinking and electrophoresis of PhK were carried out as above, but then the proteins were stained directly in gel with Coomassie blue. Prior to crosslinking for 1 min, PhK was incubated (\pm Mg^{2+}) for times varying between 0.5 and 2.0 min (indicated numerically above gel). Species that underwent Mg^{2+} -dependent crosslinking are indicated to the right of the gel. The Mg^{2+} -dependent formation of $\beta\gamma\gamma$ and $\beta\gamma\gamma_i$ is shown expanded below the gel. Masses for standard markers (Column M) are indicated in kDa to the left of the blots and gel.

identification of intrasubunit crosslinks, subscript “i,” described under Materials and Methods), and $\beta\gamma$ ($\text{mass}_{\text{Exp}} = 154$ kDa, 9.3% error). The Mg^{2+} -sensitive formation of additional conjugates of β and γ that also contained α and had apparent masses exceeding 300 kDa was also observed, but their high mass made resolution and determination of composition difficult. Intrasubunit crosslinking of the γ subunit by dibromobimane was also observed and occurred only in the presence of Mg^{2+} , forming a fast migrating band denoted as γ_i ($\text{mass}_{\text{Exp}} = 39.2$ kDa, 11.47% error) (Fig. 8). Likewise, the β subunit also underwent intrasubunit crosslinking, but this occurred both $\pm \text{Mg}^{2+}$, resulting in the generation of a band termed β_i ($\text{mass}_{\text{Exp}} = 119$ kDa, 5.3% error) that migrated slightly faster than the native β subunit (Fig. 8). Such intrasubunit crosslinking of β has been previously detected in activated forms of PhK using other crosslinkers.^{20,48}

To assure capturing structural changes induced by Mg^{2+} in the PhK complex prior to its self-association, the incubation time of $\text{PhK} \pm \text{Mg}^{2+}$ was varied from 0.5 to 2 min, after which crosslinking with dibromobimane was carried out for a fixed time of 1 min [Fig. 8(B)]. Instead of using Western blots, these crosslinked conjugates were analyzed by the less sensitive protein staining, because the high sensitivity of some of the antibodies tended to over-emphasize the relative amounts of minor conjugates. Differences in the crosslinking patterns of apo-PhK and Mg^{2+} -PhK were revealed by increased formation of the $\beta\gamma\gamma$ and $\beta\gamma\gamma_i$ conjugates with the latter conformer. Although difficult to observe with the protein stain, a small amount of γ_i could also be observed after 1 min of incubation with Mg^{2+} . These crosslinking results corroborate our physicochemical experiments and suggest that Mg^{2+} -induced rapid structural changes in the β and/or γ subunits of PhK may promote the self-association of the complex at pH 6.8, although a role for the α subunit cannot be ruled out.

To assess by crosslinking any structural changes induced in PhK by Mg^{2+} at the activating pH value of 8.2, the crosslinker DFDNB was used instead of dibromobimane, as the latter produced such extensive crosslinking under this condition that interpretation was confounded. Crosslinking of PhK by DFDNB is well-characterized and has been used to detect conformational changes induced in the complex by phosphorylation.²⁰ PhK was incubated at various times between 0.5 and 20 min $\pm \text{Mg}^{2+}$, followed by crosslinking for 1 min with DFDNB. As there was no change in crosslinking pattern over this time span, only the results from the earliest and latest time points are shown (Fig. 9). As observed previously, DFDNB formed several differentially crosslinked β dimers: $\beta\beta$ ($\text{mass}_{\text{Exp}} = 247$ kDa, 1.6% error) and two intrasubunit crosslinked dimers, $\beta\beta_i$ (230 kDa, 8.3% error) and $\beta\beta_{i2}$ (21.8%

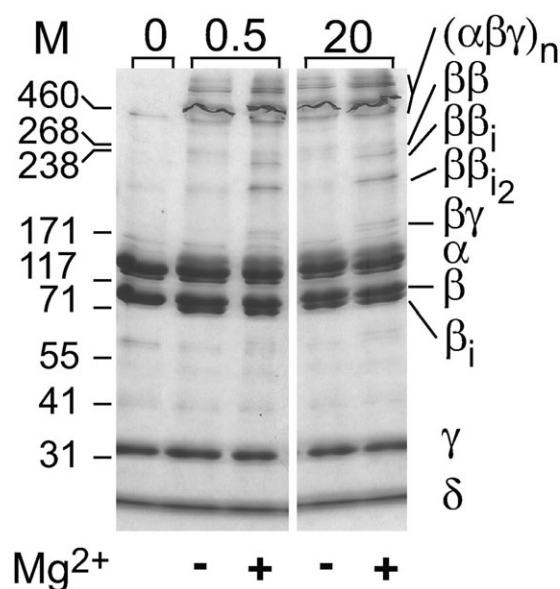


Figure 9. Crosslinking of PhK with DFDNB. Following its incubation $\pm \text{Mg}^{2+}$ for 0.5 or 20 min (indicated numerically above gel), PhK was crosslinked with DFDNB for one min at pH 8.2 (Methods). Following electrophoresis, the proteins were stained directly in gel with Coomassie blue. Subunits and conjugates are indicated to the right of the gel, with subscript i denoting intramolecular crosslinking within a conjugate. Masses for standard markers are indicated in kDa to the left of the blots and gel.

error). Intrasubunit crosslinking of the β monomer was also evident by the formation of a new band, migrating slightly faster than the native β subunit. Although the β dimers were observed after crosslinking the complex either in the presence or absence of Mg^{2+} , their extent formation increased markedly in the presence of Mg^{2+} . A $\beta\gamma$ heterodimer was also observed, but only in the presence of Mg^{2+} . That crosslinking patterns $\pm \text{Mg}^{2+}$ remained constant over 20 min agrees with our physical data showing that PhK solutions remain monodispersed with time at pH 8.2 $\pm \text{Mg}^{2+}$. Taken together, our crosslinking results with dibromobimane (pH 6.8) and DFDNB (pH 8.2) indicate that Mg^{2+} induces a conformational change in PhK that is characterized by structural changes in its β and γ subunits.

Discussion

Although the divalent cations Ca^{2+} and Mg^{2+} are both activators of PhK, they independently affect its activity. For example, Ca^{2+} is an obligatory activator under all conditions, but free Mg^{2+} further stimulates activity (i.e., total concentration exceeding that of ATP, Table I). Moreover, the two cations synergistically affect numerous properties of PhK in ways that neither cation alone can (Table I). Thus, it was not surprising to find in this study that Mg^{2+} had effects on the physical properties of PhK that were in some cases different than those observed to be

caused by Ca^{2+} in previous studies.^{25,26} The two ions also shared some effects in common, perhaps reflecting the fact that both are activators of PhK. Their similarities and differences were observed at both pH values examined.

The most striking similarity between the actions of the two cations is their effect on zeta potential. At the nonactivating pH value of 6.8, Mg^{2+} caused the zeta potential to become dramatically less negative (-32 to -6 mV) and remain constant with time. This is very similar to the effect of Ca^{2+} at this pH value and is one of the two physical properties that have been hypothesized to be associated with the activation of PhK.^{25,26} Thus, both ions cause the effective surface charge of PhK to become less negative, either from the net burial of acidic side chains or the exposure of basic ones. Neither cation had a significant effect at the activating pH value of 8.2. Another similarity in the action of the cations was their effect at pH 8.2 on the second derivative UV absorption spectra reflecting the burial of tyrosyl residues.²⁶ There was also no difference in the $\theta_{222}/\theta_{208}$ ratio caused by the binding of either ion at pH 6.8,^{25,26} at least for the first 2 min. Because of the self-association of Mg^{2+} -PhK at this pH value, measurements past 2 min were ignored.

This time-dependent self-association of PhK at pH 6.8 in the presence of Mg^{2+} is one of two major differences in the action of the two cations, as Ca^{2+} causes no such association.²⁵ This effect of Mg^{2+} was not observed at pH 8.2, although the apparent size of the enzyme complex did increase slightly. The other major difference between the ions occurred at pH 8.2, where Ca^{2+} causes a dramatic increase in the $\theta_{222}/\theta_{208}$ ratio,²⁶ but Mg^{2+} had no effect.

That both Ca^{2+} and Mg^{2+} had the similar effect of making PhK's zeta potential considerably less negative, but only Ca^{2+} increased the enzyme's $\theta_{222}/\theta_{208}$ ratio at pH 8.2, may relate to the previously discussed differences in these two cations as activators. In short, those differences are that Ca^{2+} is obligatory, whereas stimulation by free Mg^{2+} absolutely requires Ca^{2+} to be present. The biophysical changes previously observed to most closely correlate with the increase in activity associated with the binding of Ca^{2+} at increasing values of pH were the less negative zeta potential and a large increase in the $\theta_{222}/\theta_{208}$ ratio.²⁶ It is possible then that inducing the conformation giving rise to the less negative zeta potential is associated with activators in general, including Mg^{2+} , whereas the obligatory activator Ca^{2+} is also capable of further inducing the large increase in the $\theta_{222}/\theta_{208}$ ratio observed in the most active form of PhK (pH 8.2 + Ca^{2+}) and associated with decreased interactions between α -helices and β -sheets.^{31,32,34,35} It would be of interest to determine if other mechanisms for activating PhK bring about only the change in its zeta potential.

Although conformational changes in the PhK complex initiated by the binding of Ca^{2+} affect all four subunits²⁷ it is nearly certain that they emanate from the binding of Ca^{2+} to the δ subunit (intrinsic calmodulin). In the case of Mg^{2+} , the subunit most likely responsible for its binding is the catalytic γ subunit, although calmodulin also has the ability to bind Mg^{2+} ,⁴⁹ and thus cannot be ruled out. The strongest evidence suggesting that the effects of Mg^{2+} are mediated by the γ subunit is that the binding of a mAb that recognizes an epitope in the middle third of the catalytic domain was markedly enhanced by Mg^{2+} for both the isolated γ subunit and the PhK complex.¹² Moreover, free Mg^{2+} stimulates the catalytic activity of full-length and truncated forms of the γ subunit,⁵⁰⁻⁵³ as it does for PhK. A direct effect of Mg^{2+} -binding on the conformation of γ is consistent with our results showing that Mg^{2+} promotes the intramolecular crosslinking of γ within the complex by the short span (4.8 Å) crosslinker dibromobimane⁵⁴ at pH 6.8. Transmission of a Mg^{2+} -induced activating conformational signal from γ to the regulatory β subunit is consistent both with our findings herein that Mg^{2+} stimulates crosslinking by dibromobimane of γ and the regulatory β subunit in the PhK complex and with a previous report showing that γ and β are structurally coupled to each other and with enzyme activation.¹³ It should be noted that the Mg^{2+} -enhanced formation of the γ_i , $\beta\gamma\gamma$ and $\beta\gamma\gamma_i$ species by dibromobimane at pH 6.8 occurs after short incubation times prior to the aggregation of PhK. Changes in the crosslinking of the β and γ subunits by Mg^{2+} were also observed at pH 8.2 with the crosslinker DFDNB. In this case, the rate of formation of several differentially crosslinked $\beta\beta$ dimers was enhanced by the cation, and a $\beta\gamma$ dimer was observed only in its presence.

In summary, we suggest that the activator Mg^{2+} binds to the γ subunits of the PhK complex, promoting rapid, coupled structural changes in the γ and β subunits at both pH values. At pH 6.8, this activating conformational change is characterized by increased zeta potential and the formation of PhK dimers, followed slowly by more extensive self-association. For PhK at pH 8.2, Mg^{2+} -induced structural changes are manifested by the burial of Tyr residues in a more apolar environment and a slightly increased size. We conclude that the different structural changes associated with activation of PhK by Ca^{2+} and Mg^{2+} ions may be attributed to their different binding subunits within the complex.

Materials and Methods

PhK

Nonactivated PhK was purified from the psoas muscle of female New Zealand White rabbits as previously described⁹ and stored at -80°C in buffer containing

50 mM HEPES, 0.2 mM EDTA and 10% (w/v) sucrose (pH 6.8). Prior to use, frozen samples of PhK were thawed and immediately centrifuged for 30 s at 10,000g to clear the solution. Any soluble aggregates were removed by size exclusion-HPLC⁵⁵ over a BioSep SEC-S4000 column (Phenomenex) developed with a mobile phase containing 6.0 mM HEPES, 200 mM NaCl, 0.2 mM EGTA (pH 6.8) at a flow rate of 0.4 ml/min, and fractions containing only PhK hexadecamers were retained for spectroscopic analyses. Such purified enzyme solutions were subsequently dialyzed overnight against 6.0 mM HEPES, 0.2 mM EGTA at either pH 6.8 or 8.2. PhK concentrations were determined by UV₂₈₀ using an absorption coefficient of 1.24 for a 1% protein solution (Cohen 1973).⁵⁶

For analyses of PhK at different pH values, dialyzed samples were diluted with their corresponding dialysis buffers to 100 µg/mL; to achieve the same protein concentrations for Mg²⁺-PhK, enzyme solutions were diluted in the same buffers containing Mg(CH₃COO)₂·4H₂O to achieve a final free Mg²⁺ ion concentration of 4.0 mM. All techniques except electron microscopy and crosslinking utilized PhK at 100 µg/mL in 6.0 mM Hepes buffer (pH 6.8 or 8.2) and 0.2 mM EGTA.

Far UV CD spectroscopy

Far UV CD spectra were collected under constant nitrogen purge in 0.1-cm quartz cuvettes from 260 to 190 nm at 1-nm intervals with a 35 nm/min scan rate using a Jasco J-810 spectropolarimeter (Jasco). Reference spectra were subtracted from a minimum of three replicates of raw protein spectra, and analyzed using Origin Professional v.7.0 Scientific Graphing and Analysis Software (OriginLab). For time-dependent studies, PhK ± Mg²⁺ was scanned every 2 min.

Surface of shear electrostatic potential

The zeta potential at each pH value ± Mg²⁺ was determined at 25°C every 5 min for 30 min on a Brookhaven Instrument Corp ZetaPALS analyzer. Light scattering at 15° to the incident solid-state laser beam (676 nm, 25 mW) was measured to calculate the Smoluchowski approximation, which is appropriate for the typical colloid and salt concentrations that were used for these experiments.

Optical density measurements

The optical density at 360 nm of Mg²⁺-PhK was obtained on a DU 800 spectrophotometer (Beckman Coulter) from zero to 120 min at different pH values to monitor any aggregation behavior. Studies were conducted in capped quartz cuvettes at 25°C.

DLS

The aggregation behavior of Mg²⁺-PhK as a function of time was monitored by DLS. PhK was prepared

immediately before the experiment. Measurements were recorded at 25°C in a light scattering instrument [Nicom Particle Sizing System Model 370 (Saint Barbara, CA) equipped with a 35-milliwatt diode-pumped laser ($\lambda = 632.8$ nm)]. The scattering light was monitored at 90° to the incident beam, and the DLS data were accumulated and analyzed with the CW 388 Application Version 1.55 of the instrument.

Negatively stained electron microscopy

Images of stained PhK were recorded at a magnification of 60,000× using minimal-dose protocols with a JEOL 1200EX electron microscope. HPLC-purified, dialyzed PhK was diluted to a final concentration of 10 nM, incubated with 4.0 mM Mg²⁺ ions for 30 s, and immediately prepared for electron microscopy by brief adsorption to plasma-discharged carbon films on 300 mesh copper support grids. The samples were rapidly washed with distilled water and stained with 2% uranyl acetate. Micrographs were digitized with a Eurocore HiScan densitometer using a 30 µm pixel size and stored as 16-bit files. Image analyses were performed on a Compaq alpha workstation with SPIDER and WEB software packages.⁴⁵ Individual molecules of PhK were identified by visual inspection of WEB displays and manually selected.

Second derivative UV absorption spectroscopy

High resolution UV absorption spectra were collected on an Agilent 8453 diode-array spectrophotometer (Agilent Technologies). Spectra were analyzed between 240 and 310 nm with 1.0-nm increments. Studies were conducted in 1-cm quartz cuvettes and a 5-min temperature equilibration time was incorporated before collection of each spectrum. Second derivatives of individual spectra were calculated applying a nine-point filter and fifth-degree Savitsky-Golay polynomial fitted to a cubic function with a 99-point interpolation per raw data point using the UV-Visible Chemstation software suite (Agilent Technologies). Second derivative peak minima were assigned by peak picking with the OriginPro software program.

Chemical crosslinking

Prior to crosslinking with DFDNB, PhK was incubated ± 4.2 mM Mg²⁺ for times progressing from 0.5 to 20 min at pH 8.2 in 50 mM Hepes buffer containing 0.2 mM EGTA. The complex was then crosslinked essentially as described,^{14,57} with cross-linking initiated by addition of DFDNB and carried out at 30°C for 1.0 min. Final concentrations of PhK ($\alpha\beta\gamma\delta$ protomer) and DFDNB in the reaction were 0.47 and 117.5 µM, respectively. The reaction was terminated by adding an equal volume of SDS buffer [0.125 M Tris (pH 6.8), 20% glycerol, 5% β-mercaptoethanol, 4% SDS],

followed by brief vortexing. The PhK subunits were separated on 6–18% linear gradient polyacrylamide gels and stained with Coomassie Blue. Western blotting was performed on PVDF membranes with subunit-specific mAbs as previously described.⁵⁷ Cross-linked subunits or conjugates thereof were identified by cross-reactivity against these monoclonal antibodies and their apparent mass judged by SDS-PAGE. Intrasubunit crosslinking was revealed by the formation of a new band that migrated faster than the non-modified subunit, but cross-reacted only with the antibody specific for that subunit. An intramolecularly crosslinked protein cannot fully extend in the presence of SDS, thus its Stokes radius is decreased and its migration in the gel increased.

All crosslinking reactions were performed at least twice using different preparations of PhK. Crosslinking with dibromobimane and Western blotting were carried out as above, except in 50 mM Hepes, pH 6.8. Final concentrations of PhK ($\alpha\beta\gamma\delta$ protomer) and dibromobimane in the reaction were 0.47 and 23.5 μ M, respectively.

References

- Krebs EG, Fischer EH (1956) The phosphorylase b to a converting enzyme of rabbit skeletal muscle. *Biochim Biophys Acta* 20:150–157.
- Brushia RJ, Walsh DA (1999) Phosphorylase kinase: the complexity of its regulation is reflected in the complexity of its structure. *Front Biosci* 4:D618–D641.
- Chelala CA, Torres HN (1968) Activation of muscle phosphorylase b kinase by Mg^{++} . *Biochem Biophys Res Commun* 32:704–709.
- Kim G, Graves DJ (1973) On the hysteretic response of rabbit skeletal muscle phosphorylase kinase. *Biochemistry* 12:2090–2095.
- Villar-Palasi C, Wei SH (1970) Conversion of glycogen phosphorylase b to a by non-activated phosphorylase b kinase: an in vitro model of the mechanism of increase in phosphorylase a activity with muscle contraction. *Proc Natl Acad Sci USA* 67:345–350.
- Singh TJ, Akatsuka A, Huang KP (1982) The regulatory role of Mg^{2+} on rabbit skeletal muscle phosphorylase kinase. *Arch Biochem Biophys* 218:360–368.
- Clerch LB, Huijing F (1972) The role of magnesium in muscle phosphorylase kinase activity. *Biochim Biophys Acta* 268:654–662.
- Kilimann M, Heilmeyer LM, Jr (1977) The effect of Mg^{2+} on the Ca^{2+} -binding properties of non-activated phosphorylase kinase. *Eur J Biochem* 73:191–197.
- Xu YH, Wilkinson DA, Carlson GM (1996) Divalent cations but not other activators enhance phosphorylase kinase's affinity for glycogen phosphorylase. *Biochemistry* 35:5014–5021.
- Ayers NA, Nadeau OW, Read MW, Ray P, Carlson GM (1998) Effector-sensitive cross-linking of phosphorylase b kinase by the novel cross-linker 4-phenyl-1,2,4-triazoline-3,5-dione. *Biochem J* 331:137–141.
- Trempe MR, Carlson GM (1987) Phosphorylase kinase conformers. Detection by proteases. *J Biol Chem* 262:4333–4340.
- Wilkinson DA, Fitzgerald TJ, Marion TN, Carlson GM (1999) Mg^{2+} induces conformational changes in the catalytic subunit of phosphorylase kinase, whether by itself or as part of the holoenzyme complex. *J Protein Chem* 18:157–164.
- Wilkinson DA, Norcum MT, Fitzgerald TJ, Marion TN, Tillman DM, Carlson GM (1997) Proximal regions of the catalytic gamma and regulatory beta subunits on the interior lobe face of phosphorylase kinase are structurally coupled to each other and with enzyme activation. *J Mol Biol* 265:319–329.
- Singh TJ, Wang JH (1977) Effect of Mg^{2+} concentration on the cAMP-dependent protein kinase-catalyzed activation of rabbit skeletal muscle phosphorylase kinase. *J Biol Chem* 252:625–632.
- Yu JS, Lee SC, Yang SD (1995) Effect of Mg^{2+} concentrations on phosphorylation/activation of phosphorylase b kinase by cAMP/ Ca^{2+} -independent, autophosphorylation-dependent protein kinase. *J Protein Chem* 14:747–752.
- Carlson GM, King, MM (1982) Aggregation of phosphorylase kinase induced by Ca^{2+} and Mg^{2+} . *Federation Proc* 41:869.
- Chebotareva NA, Meremyanin AV, Makeeva VF, Kurganov BI (2006) Self-association of phosphorylase kinase under molecular crowding conditions. *Prog Colloid Polymer Sci* 131:83–92.
- Chebotareva NA, Meremyanin AV, Makeeva VF, Livanova NB, Kurganov BI (2008) Cooperative self-association of phosphorylase kinase from rabbit skeletal muscle. *Biophys Chem* 133:45–53.
- King MM, Carlson GM (1981) Synergistic activation by Ca^{2+} and Mg^{2+} as the primary cause for hysteresis in the phosphorylase kinase reactions. *J Biol Chem* 256:11058–11064.
- Fitzgerald TJ, Carlson GM (1984) Activated states of phosphorylase kinase as detected by the chemical cross-linker 1,5-difluoro-2,4-dinitrobenzene. *J Biol Chem* 259:3266–3274.
- King MM, Carlson GM (1981) Synergistic effect of Ca^{2+} and Mg^{2+} in promoting an activity of phosphorylase kinase that is insensitive to ethylene glycol bis(beta-aminoethyl ether)-N,N'-tetraacetic acid. *Arch Biochem Biophys* 209:517–523.
- Steiner RF, Marshall L (1982) Synergistic effect of Ca^{2+} and Mg^{2+} upon the interaction of phosphorylase kinase with glycogen. *Biochim Biophys Acta* 707:38–45.
- Andreeva IE, Makeeva VF, Kurganov BI, Chebotareva NA, Livanova NB (1999) Kinetics of the interaction of rabbit skeletal muscle phosphorylase kinase with glycogen. *Biochemistry (Mosc)* 64:159–168.
- Andreeva IE, Makeeva VF, Kurganov BI, Chebotareva NA, Livanova NB (1999) A tentative mechanism of the ternary complex formation between phosphorylase kinase, glycogen phosphorylase b and glycogen. *FEBS Lett* 445:173–176.
- Priddy TS, Middaugh CR, Carlson GM (2007) Electrostatic changes in phosphorylase kinase induced by its obligatory allosteric activator Ca^{2+} . *Protein Sci* 16:517–527.
- Liu W, Priddy TS, Carlson GM (2008) Physicochemical changes in phosphorylase kinase associated with its activation. *Protein Sci* 17:2111–2119.
- Nadeau OW, Carlson GM (2012) Methods for detecting structural changes in large protein complexes. *Methods in molecular biology*, Vol. 796 (Allostery: Methods and Protocols; Fenton AW, Ed), Totowa, NJ: Humana Press, pp 117–132.
- Pickett-Gies CA, Walsh DA. Phosphorylase kinase. In: Boyer PD, Krebs EG, Eds. (1986) *The Enzymes*, Vol. IX-VII. Orlando, FL: Academic Press, pp 395–459.

29. Chan KF, Graves DJ (1982) Rabbit skeletal muscle phosphorylase kinase. Catalytic and regulatory properties of the active alpha gamma delta and gamma delta complexes. *J Biol Chem* 257:5948–5955.
30. Kee SM, Graves DJ (1986) Isolation and properties of the active gamma subunit of phosphorylase kinase. *J Biol Chem* 261:4732–4737.
31. Levitt M, Chothia C (1976) Structural patterns in globular proteins. *Nature* 261:552–558.
32. Chothia C, Levitt M, Richardson D (1977) Structure of proteins: packing of alpha-helices and pleated sheets. *Proc Natl Acad Sci USA* 74:4130–4134.
33. Manavalan P, Johnson WC (1983) Sensitivity of circular dichroism to protein tertiary structure class. *Nature* 305:831–832.
34. Arnold GE, Day LA, Dunker AK (1992) Tryptophan contributions to the unusual circular dichroism of fd bacteriophage. *Biochemistry* 31:7948–7956.
35. Park K, Flynn GC, Rothman JE, Fasman GD (1993) Conformational change of chaperone Hsc70 upon binding to a decapeptide: a circular dichroism study. *Protein Sci* 2:325–330.
36. Hunter RJ. 1981. Zeta potential in colloid science: principles and applications. London, New York: Academic Press, pp 17–32.
37. McNeil-Watson F, Tscharnuter W, Miller J (1998) A new instrument for the measurement of very small electrophoretic mobilities using phase analysis light scattering (PALS). *Colloids Surf A* 140:53–57.
38. Tsumoto K, Umetsu M, Kumagai I, Ejima D, Arakawa T (2003) Solubilization of active green fluorescent protein from insoluble particles by guanidine and arginine. *Biochem Biophys Res Commun* 312:1383–1386.
39. Ausar SF, Foubert TR, Hudson MH, Vedvick TS, Middaugh CR (2006) Conformational stability and disassembly of Norwalk virus-like particles. Effect of pH and temperature. *J Biol Chem* 281:19478–19488.
40. Benjwal S, Verma S, Rohm KH, Gursky O (2006) Monitoring protein aggregation during thermal unfolding in circular dichroism experiments. *Protein Sci* 15: 635–639.
41. Ausar SF, Rexroad J, Frolov VG, Look JL, Konar N, Middaugh CR (2005) Analysis of the thermal and pH stability of human respiratory syncytial virus. *Mol Pharm* 2:491–499.
42. Nadeau OW, Gogol EP, Carlson GM (2005) Cryoelectron microscopy reveals new features in the three-dimensional structure of phosphorylase kinase. *Protein Sci* 14:914–920.
43. Priddy TS, MacDonald BA, Heller WT, Nadeau OW, Trehella J, Carlson GM (2005) Ca²⁺-induced structural changes in phosphorylase kinase detected by small-angle X-ray scattering. *Protein Sci* 14:1039–1048.
44. Norcum MT, Wilkinson DA, Carlson MC, Hainfeld JF, Carlson GM (1994) Structure of phosphorylase kinase. A three-dimensional model derived from stained and unstained electron micrographs. *J Mol Biol* 241: 94–102.
45. Frank J, Radermacher M, Penczek P, Zhu J, Li Y, Ladjadj M, Leith A (1996) SPIDER and WEB: processing and visualization of images in 3D electron microscopy and related fields. *J Struct Biol* 116:190–199.
46. Mach H, Middaugh CR (1994) Simultaneous monitoring of the environment of tryptophan, tyrosine, and phenylalanine residues in proteins by near-ultraviolet second-derivative spectroscopy. *Anal Biochem* 222: 323–331.
47. Demchenko AP. Derivative spectroscopy of aromatic amino acids and proteins (1986) Ultraviolet spectroscopy of proteins. New York: Springer-Verlag, Berlin, pp 121–135.
48. Nadeau OW, Wyckoff GJ, Paschall JE, Artigues A, Sage J, Villar MT, Carlson GM (2008) CrossSearch, a user-friendly search engine for detecting chemically cross-linked peptides in conjugated proteins. *Mol Cell Proteomics* 7:739–749.
49. Grabarek Z (2011) Insights into modulation of calcium signaling by magnesium in calmodulin, troponin C and related EF-hand proteins. *Biochim Biophys Acta* 1813: 913–921.
50. Kee SM, Graves DJ (1987) Properties of the gamma subunit of phosphorylase kinase. *J Biol Chem* 262: 9448–9453.
51. Farrar YJ, Carlson GM (1991) Kinetic characterization of the calmodulin-activated catalytic subunit of phosphorylase kinase. *Biochemistry* 30:10274–10279.
52. Cox S, Johnson LN (1992) Expression of the phosphorylase kinase gamma subunit catalytic domain in *Escherichia coli*. *Protein Eng* 5:811–819.
53. Huang CY, Yuan CJ, Livanova NB, Graves DJ (1993) Expression, purification, characterization, and deletion mutations of phosphorylase kinase gamma subunit: identification of an inhibitory domain in the gamma subunit. *Mol Cell Biochem* 127–128:7–18.
54. Green NS, Reisler E, Houk KN (2001) Quantitative evaluation of the lengths of homobifunctional protein cross-linking reagents used as molecular rulers. *Protein Sci* 10:1293–1304.
55. Traxler KW, Norcum MT, Hainfeld JF, Carlson GM (2001) Direct visualization of the calmodulin subunit of phosphorylase kinase via electron microscopy following subunit exchange. *J Struct Biol* 135:231–238.
56. Cohen P (1973) The subunit structure of rabbit-skeletal-muscle phosphorylase kinase, and the molecular basis of its activation reactions. *Eur J Biochem* 34:1–14.
57. Nadeau OW, Anderson DW, Yang Q, Artigues A, Paschall JE, Wyckoff GJ, McClintock JL, Carlson GM (2007) Evidence for the location of the allosteric activation switch in the multisubunit phosphorylase kinase complex from mass spectrometric identification of chemically crosslinked peptides. *J Mol Biol* 365: 1429–1445.